

The Liquid-Junction Potential at the Contact of Two Immiscible Electrolyte Solutions in the Absence of Supporting Electrolytes Reference Electrodes Reversible to Alkylammonium Ions and Tetraphenylborate Ion in Nitrobenzene

Takashi KAKIUCHI and Mitsugi SENDA*

Department of Agricultural Chemistry, Faculty of Agriculture, Kyoto University,
Sakyo-ku, Kyoto 606

(Received March 4, 1987)

The liquid-junction potentials between two immiscible electrolyte solutions have been studied for the interface: $R^+TPB^-(\text{nitrobenzene})/R^+X^-(\text{water})$ and $R^+TPB^-(\text{nitrobenzene})/Li^+TPB^-(\text{water})$, where R^+ is a tetraalkylammonium ion, TPB^- is tetraphenylborate ion, and X^- is a halide ion. These interfaces may be seen as a simplest form of either a liquid ion-exchange membrane ion-selective electrode sensing the activity of the ion in the aqueous phase or a reference electrode of a liquid membrane type reversible to the ion in the nonaqueous phase. The effects of the cationic species(R^+), the anionic species(X^-) and the concentration of the electrolytes on the electrical potential difference developed at the interface have been studied. These properties of the interfaces were compared with a simplified theoretical treatment of the liquid-junction potential between the two immiscible solutions. The theory can predict the basic features of the system by knowing the standard ion-transfer potentials and the diffusion coefficients of the relevant ions as well as its concentration. In the concentration range where a significant deviation from the Nernstian response of the liquid-junction potential occurred, the diffusion potential has been demonstrated to contribute significantly to the liquid-junction potential.

In the study of the double layer structure of the interface between two immiscible electrolyte solutions(ITIES) and the electrochemistry of charge transfer at the interface, large hydrophobic ions such as tetrabutylammonium ion(TBA^+) and tetraphenylborate ion(TPB^-) are used for a supporting electrolyte in the nonaqueous phase.^{1a, b)} In order that the electrical potential difference across the interface be well defined, it is desirable to use a reference electrode which is reversible to one of such organic ions in the nonaqueous phase. For this purpose, an aqueous solution containing the ion which is the same as one of the ions in the nonaqueous phase has been usually employed;^{1a, b)} the aqueous phase and the nonaqueous phase in contact form a nonpolarized interface through which the common ion works as a potential-determining ion. When all other ions are not transferable across the interface, there exists a so called contact equilibrium²⁾ between the two phases and there is no net flow of ions through the interface. The potential difference between the two phases is then represented by the Nernst equation with respect to the common ion. When an ion other than the potential-determining ion, e.g., a counter ion of the potential-determining ion, is also appreciably transferable between the two phases, a net flow of the ions across the interface generally occurs even at zero-current condition until the final distribution equilibrium is attained.

The potential difference between two immiscible electrolyte solutions has been analyzed in detail by Hung³⁾ in the case where the distribution equilibrium of the ions between the two phases is established. He

derived the equations which predict the distribution potential by knowing the initial concentrations and the standard ion-transfer potentials of the ions as well as the volumes of the two phases. However, in practice, the reference electrodes with ITIES are not always used under the condition of ultimate distribution equilibrium throughout the phases, and the potential difference across the interface is yet quite stable irrespective of the volumes of the two solutions shortly after the initial contact of these solutions. Therefore, it is necessary to study experimentally as well as theoretically the electrical potential difference between two immiscible electrolyte solutions without resorting to the assumption of the distribution equilibrium over the two phases in contact. This is the purpose of this study. We have previously presented the theory of the mixed ion-transfer potential at the ITIES in the presence of the supporting electrolytes in both phases.⁴⁾ We report here the theoretical treatment as well as the experimental study of the liquid-junction potential (l.j.p.) of the type: $R^+TPB^-(\text{nitrobenzene})/R^+X^-(\text{water})$ and $R^+TPB^-(\text{nitrobenzene})/Li^+TPB^-(\text{water})$, where R^+ is a tetraalkylammonium ion, TPB^- is tetraphenylborate ion, and X^- is a halide ion. The interfaces of these systems may also be seen as the interface between a liquid membrane and a sample solution in the liquid-membrane ion-selective electrode. Accordingly, this study will also provide us with insight into the basic properties of ion-selective electrodes.

Theoretical

Let us consider the electrical potential difference that develops across a plane interface when we bring into contact a semi-infinite aqueous phase containing 1:1 electrolyte K_1A_1 with a semi-infinite nonaqueous (oil) phase containing 1:1 electrolyte K_1A_2 , where K and A denote a cation and an anion, respectively. In most of the cases encountered in practice, the ion transfer of one of these three ionic species can be neglected.³⁾ In the following, we consider only the case where only two ionic species K_1 and A_1 are transferable across the interface. The K_1 and A_1 may then be considered as a primary ion and an interfering ion, respectively. For the sake of simplicity, we assume the complete dissociations of K_1A_2 in the oil phase and of K_1A_1 in both phases and neglect the activity coefficients of the relevant ions. Let the x -axis be chosen normal to the interface, where $x=0$, and be directed from the oil toward the aqueous phase. The flux of an ion in each phase may be represented by the Nernst-Planck equation:

$$f_i^\alpha = -D_i^\alpha \frac{\partial c_i^\alpha}{\partial x} - \frac{z_i F}{RT} D_i^\alpha c_i^\alpha \frac{\partial \varphi^\alpha}{\partial x}, \quad (1)$$

where f is the flux, D is the diffusion coefficient, c is the concentration of the ion i , φ is the electrical potential (inner potential), x is the distance normal to the plane, z_i is the charge number of ion, and F , R , and T have the usual meanings. The superscript α ($\alpha=O$ or W) denotes the phase, whereas the subscript i ($i=K_1$, A_1 , or A_2) the ionic species. Since there are three ionic species in the oil phase when the ion transfer of the ion A_1 takes place, the diffusion-migration problem in the oil phase is not solved analytically. We treat here the case where the concentration of the interfering ion (A_1) in the oil phase is so small that the migration of A_1 in the oil phase is negligible. This approximation holds as long as the deviation from the Nernstian response is small.

When the condition

$$D_{K_1}^O c_{K_1}^O + D_{A_2}^O c_{A_2}^O \gg D_{A_1}^O c_{A_1}^O \quad (2)$$

is fulfilled, we obtain the following equations for the mass transfer of the ions in the oil phase (See Appendix 1):

$$\frac{\partial c_{K_1}^O}{\partial t} = \mathcal{D}_1^O \frac{\partial^2 c_{K_1}^O}{\partial x^2} + \mathcal{D}_2^O \frac{\partial^2 c_{A_1}^O}{\partial x^2} \quad (3)$$

and

$$\frac{\partial c_{A_1}^O}{\partial t} = D_{A_1}^O \frac{\partial^2 c_{A_1}^O}{\partial x^2} \quad (4)$$

where

$$\mathcal{D}_1^O = \frac{2D_{K_1}^O D_{A_2}^O}{D_{K_1}^O + D_{A_2}^O} \quad (5)$$

and

$$\mathcal{D}_2^O = \frac{D_{K_1}^O (D_{A_1}^O - D_{A_2}^O)}{D_{K_1}^O + D_{A_2}^O} \quad (6)$$

Similarly, for the aqueous phase we may write

$$\frac{\partial c_{K_1}^W}{\partial t} = \mathcal{D}^W \frac{\partial^2 c_{K_1}^W}{\partial x^2} \quad (7)$$

where

$$\mathcal{D}^W = \frac{2D_{K_1}^W D_{A_1}^W}{D_{K_1}^W + D_{A_1}^W} \quad (8)$$

The initial and boundary conditions for the differential Eqs. 3, 4, and 7 are:

$$c_{K_1}^O = b_{K_1A_2}^O \quad (t=0, x<0) \quad (9)$$

$$c_{A_1}^O = 0$$

$$c_{K_1}^W = b_{K_1A_1}^W \quad (t=0, x>0) \quad (10)$$

$$c_{K_1}^O = b_{K_1A_2}^O \quad (t>0, x=-\infty) \quad (11)$$

$$c_{A_1}^O = 0$$

$$c_{K_1}^W = b_{K_1A_1}^W \quad (t>0, x=+\infty) \quad (12)$$

Here, $b_{K_1A_2}^O$ and $b_{K_1A_1}^W$ are the bulk concentrations of the electrolyte K_1A_2 in the oil phase and K_1A_1 in the aqueous phase.

The continuity of the flux for K_1 at the interface, $f_{K_1}^O|_{x=0} = f_{K_1}^W|_{x=0}$, leads to

$$\begin{aligned} [-D_{A_1}^O + t_{A_1}^W (D_{K_1}^O + D_{A_1}^O)] \frac{\partial c_{A_1}^O}{\partial x} \Big|_{x=0} &= -\mathcal{D}^W \frac{\partial c_{A_1}^W}{\partial x} \Big|_{x=0} \\ &+ 2t_{A_1}^W D_{K_1}^O \frac{\partial c_{K_1}^O}{\partial x} \Big|_{x=0} \end{aligned} \quad (13)$$

where

$$t_{A_1}^W = \frac{D_{A_1}^W}{D_{K_1}^W + D_{A_1}^W} \quad (14)$$

Furthermore, since the ion-transfer reaction at the oil-water interface is usually a fast process,⁵⁾ the surface concentrations of the K_1 in both phases are related through the Nernst equation:

$$p = \frac{c_{K_1}^O(0, t)}{c_{K_1}^W(0, t)} = \exp \left[\frac{F}{RT} (\Delta_0^W \varphi - \Delta_0^O \varphi_{K_1}^O) \right] \quad (15)$$

Similarly, for the anion A_1 ,

$$q = \frac{c_{A_1}^O(0, t)}{c_{A_1}^W(0, t)} = \exp \left[-\frac{F}{RT} (\Delta_0^W \varphi - \Delta_0^O \varphi_{A_1}^O) \right] \quad (16)$$

In Eqs. 15 and 16, $\Delta_0^W \varphi$ is the inner potential of the aqueous phase with respect to that in the oil phase. It is the quantity usually called the interfacial potential or phase-boundary potential.⁴⁾ $\Delta_0^W \varphi_{K_1}^O$ and $\Delta_0^O \varphi_{A_1}^O$ are the standard ion-transfer potentials for K_1 and A_1 .¹⁾

Solving the Eqs. 3, 4, and 7 under these initial and boundary conditions, Eqs. 9–16, we finally obtain for the interfacial potential at zero current, $\Delta_0^w \varphi_{\text{interfacial}, i=0}$ (See Appendix 2):

$$\Delta_0^w \varphi_{\text{interfacial}, i=0} = \Delta_0^w \varphi_{K1}^w + \frac{RT}{F} \ln \left\{ \frac{1}{2} \left[\frac{b_{C_{K1A2}}^O}{b_{C_{K1A1}}^w} + \left(\frac{b_{C_{K1A2}}^O}{b_{C_{K1A1}}^w} \right)^2 + 4\alpha\xi \right]^{1/2} \right\} \quad (17)$$

where

$$\alpha = \left(\frac{D_{A1}^O}{\mathcal{D}^w} \right)^{1/2} \frac{b_{C_{K1A2}}^O}{b_{C_{K1A1}}^w} + \frac{1}{2} \left(\frac{\mathcal{D}_1^O}{D_{A1}^O} \right)^{1/2} \left(1 + \frac{D_{A1}^O}{D_{K1}^O} \right) + \frac{\mathcal{D}_2^O}{D_{A1}^O + (D_{A1}^O \mathcal{D}_1^O)^{1/2}} \quad (18)$$

and

$$\xi = \exp \left[\frac{F}{RT} (\Delta_0^w \varphi_{A1}^O - \Delta_0^w \varphi_{K1}^O) \right] \quad (19)$$

The interfacial potential depends on the concentration ratio $b_{C_{K1A2}}^O/b_{C_{K1A1}}^w$, the difference in the values of the standard ion-transfer potentials, and the diffusion coefficients of the relevant ions in both phases, which actually enter into Eq. 17 through the ratio D_{K1}^O/D_{A1}^O , D_{A1}^O/D_{A1}^w , D_{A2}^O/D_{A1}^O , and D_{A1}^O/D_{K1}^O . When the condition

$$\left(\frac{b_{C_{K1A2}}^O}{b_{C_{K1A1}}^w} \right)^2 \gg 4\alpha\xi \quad (20)$$

is fulfilled, Eq. 17 reduces to

$$\Delta_0^w \varphi_{\text{interfacial}, i=0} = \Delta_0^w \varphi_{K1}^O + \frac{F}{RT} \ln \frac{b_{C_{K1A2}}^O}{b_{C_{K1A1}}^w} \quad (21)$$

Namely, as long as the $b_{C_{K1A1}}^w$ is sufficiently small, the ITIES reveals the Nernstian response with respect to the concentration of the ion K_1 , even when ξ is appreciably large, i.e., A_1 is relatively hydrophobic.

Equation 17 has a form similar to the equation derived by Hung (Eq. 34 in Ref. 3) assuming that the distribution equilibrium is established throughout the two phases and the volumes of the two phases are equal. In Hung's equation, α is given by

$$\alpha = 1 + \frac{c_{K1A2}^O}{c_{K1A1}^w} \quad (22)$$

where c_{K1A1}^O and c_{K1A1}^w are the initial concentrations of electrolytes. When all the diffusion constants of the ions are equal in both phases, Eq. 18 reduces to Eq. 22. However, its physical meanings are different from those of Eq. 17. Equation 17 contains the terms involving the diffusion coefficients of the relevant ions, reflecting the importance of the transport processes of the ions. The advantage of Eq. 17 over Hung's equation is that one need not assume any size of the volume for the two solutions nor the establishment of the distribution equilibrium throughout the two phases, which may rarely occur in

practical cases.

In addition to the interfacial potential, there exists the diffusion potential on each side of the interface insofar as the system is not at equilibrium. This diffusion potential becomes significant when the transfer of K_1A_1 from the aqueous phase to the oil phase becomes discernable. The diffusion potential in the oil phase, φ_{diff}^O , and that in the aqueous phase, φ_{diff}^w , may be written as (See Appendix 2):

$$\varphi_{\text{diff}}^O = \frac{RT}{F} (1 - 2t_{K1}^O) \ln \frac{Ap'}{b_{C_{K1A2}}^O} \quad (23)$$

and

$$\varphi_{\text{diff}}^w = \frac{RT}{F} (1 - 2t_{A1}^w) \ln \frac{A}{b_{C_{K1A1}}^w} \quad (24)$$

where

$$A = \frac{N b_{C_{K1A2}}^O + (\mathcal{D}^w)^{1/2} b_{C_{K1A1}}^w}{Mq' + Np' + (\mathcal{D}^w)^{1/2}} \quad (25)$$

$$M = (D_{A1}^O)^{1/2} - t_{A1}^w \left[\frac{D_{K1}^O + D_{A1}^O}{(D_{A1}^O)^{1/2}} + \frac{2D_{K1}^O \mathcal{D}_2^O}{D_{A1}^O (\mathcal{D}_1^O)^{1/2} + \mathcal{D}_1^O (D_{A1}^O)^{1/2}} \right] \quad (26)$$

$$N = 2t_{A1}^w D_{K1}^O / (\mathcal{D}_1^O)^{1/2} \quad (27)$$

$$t_{K1}^O = D_{K1}^O / (D_{K1}^O + D_{A2}^O)$$

and p' and q' are p and q at zero current. The total potential difference between the two phases at zero current, i.e., the l.j.p. at zero current, $\Delta_0^w \varphi_{i=0}$, is generally given by

$$\Delta_0^w \varphi_{i=0} = \varphi_{\text{diff}}^O + \Delta_0^w \varphi_{\text{interfacial}, i=0} + \varphi_{\text{diff}}^w \quad (28)$$

It is noted that if we take account of the migration of A_1 ion in the oil phase, the diffusion potential could be much larger than expected from Eq. 23.

Experimental

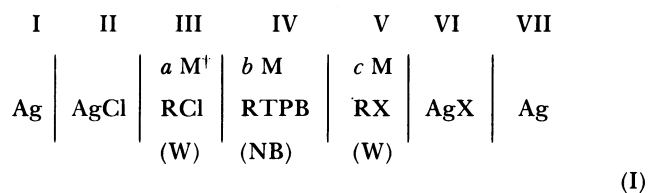
Reagent-grade nitrobenzene was treated with active alumina and then equilibrated with twice distilled water. Tetraphenylborate salts of tetrahexyl-(THA⁺), tetrapentyl-(TPnA⁺), tetrabutyl-, and tetrapropylammonium (TPrA⁺) ions were prepared from sodium tetraphenylborate (Dojin Lab., Japan) and corresponding alkylammonium halides of reagent grade as described previously.⁶ Reagent grade tetrabutylammonium chloride and tetrapropylammonium chloride were recrystallized from acetone-ether mixture. The aqueous solutions of these salts were stirred in the presence of AgCl powder to remove a trace amount of bromide and/or iodide ions. Lithium tetraphenylborate (LiTPB) was prepared from sodium tetraphenylborate.⁷ The stock solution of 0.0705 mol dm⁻³ LiTPB contained 0.001 mol dm⁻³ lithium hydroxide to prevent the decomposition of LiTPB. The concentration of LiTPB was determined by titration of the solution with zephiramine.⁸

The electromotive force of the cell was measured with a Keithley 616 electrometer. The cell was made in a U-shaped

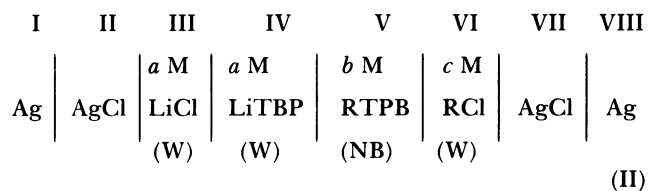
poly(tetrafluoroethylene) tubing of 9 mm inner diameter and 10 cm tall. About 8 ml of a nitrobenzene solution was first put into the tubing and then a few milliliter of aqueous solution were added onto the nitrobenzene solution in each leg of the cell. Appropriate reference electrodes were then immersed into the aqueous solutions. The liquid-liquid contact in a reference electrode, if necessary, was made via a glass frit when the solvent is water, or a poly(vinyl chloride) gel of nitrobenzene solution when the solvent is nitrobenzene. The cell was immersed in a water bath at $25 \pm 0.1^\circ\text{C}$. The emf measurements were started immediately after the contact of the aqueous and nitrobenzene solutions.

Results and Discussion

Nitrobenzene-Water Interface Reversible to Large Tetraalkylammonium Ions. Effect of Cationic Species: The emf response of the interface, $\text{RCl(W)}/\text{RTPB(NB)}$, to $c_{\text{RCl}}^{\text{W}}$ was measured at $c_{\text{RTPB}}^{\text{O}} = \text{const.}$ for $\text{R} = \text{TPrA}^+$, TBA^+ , TPnA^+ , and THA^+ . The following two types of the cell were used;



and



The interface between the phases IV and V in the cell (I) and that between V and VI in the cell (II) are the nonpolarized interfaces at which the l.j.p. we are concerned with resides. The cell (I) was used for $\text{R} = \text{TPrA}^+$ ($a=1$, $b=1$, and $c=1-500 \text{ mmol dm}^{-3}$) and TBA^+ ($a=10$, $b=50$, and $c=0.1-200 \text{ mmol dm}^{-3}$), and the cell(II) for $\text{R} = \text{TPnA}^+$ ($a=1$, $b=100$, and $c=0.1-100 \text{ mmol dm}^{-3}$) and THA^+ ($a=1$, $b=40$, and $c=0.02-2 \text{ mmol dm}^{-3}$). Since the nitrobenzene phase was thick, the potential between the phases III and IV in the cell (I) and that between IV and V in the cell(II) remain unchanged with the change of $c_{\text{RCl}}^{\text{W}}$. The l.j.p. across the phases III and IV in the cell(II) is also constant. The change in the potential difference between phases V and VI in (I) and that between phases VI and VII in the cell(II) with the change of $c_{\text{RCl}}^{\text{W}}$ were calculated assuming the Nernstian response of the Ag/AgCl electrodes to the Cl^- ion. The activity coefficients of RCl 's were estimated by using the Davies equation.⁹ These calculated values were added

[†] 1 M = 1 mol dm^{-3} .

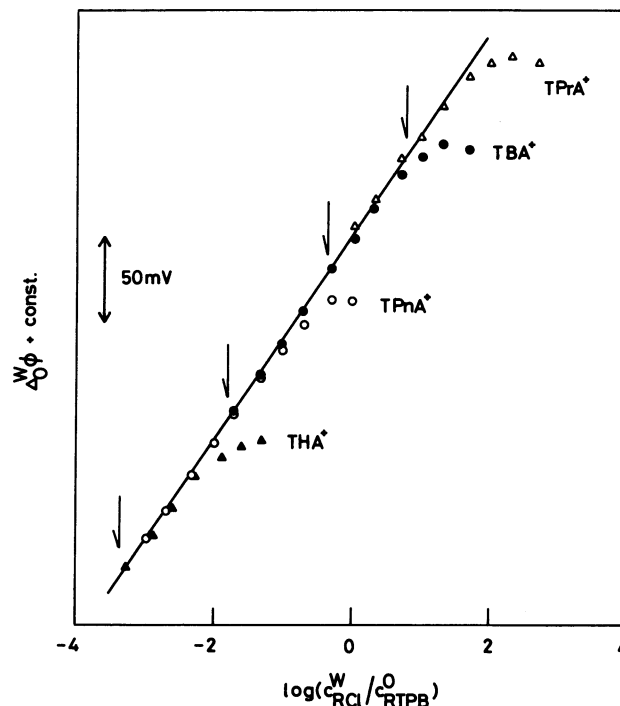
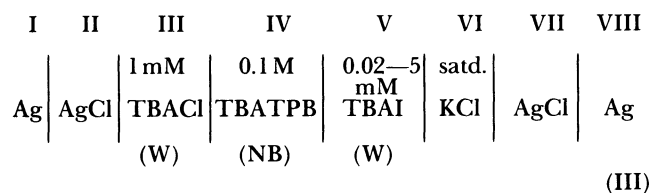


Fig. 1. Change of the liquid junction potentials for the system: $\text{RTPB}(\text{nitrobenzene})/\text{RCl}(\text{water})$, where $\text{R} = \text{tetrapropylammonium}(\text{TPrA}^+)$, $\text{tetrabutylammonium}(\text{TBA}^+)$, $\text{tetrapentylammonium}(\text{TPnA}^+)$, or $\text{tetrahexylammonium ion}(\text{THA}^+)$.

to the corresponding emf values to obtain the change of the l.j.p. at the interface. The resultant variation of the l.j.p. values was plotted against the logarithm of the concentration ratio, $\log(c_{\text{RCl}}^{\text{W}}/c_{\text{RTPB}}^{\text{O}})$. These curves were shifted vertically so that their linear portions were superimposed upon each other, eliminating the difference in the emf values due to the different reference electrode included in each cell. Figure 1 indicates that TPrA^+ has the largest concentration range of the Nernstian response. With the increase of the alkyl-chain length, the Nernstian region becomes narrower, as is expected from the theoretical treatment given above, because the increase in the hydrophobicity of the cation gives rise to the increase in ξ in Eq. 17 (see also Eq. 19). The arrows in Fig. 1 indicate the predicted points, where the curves deviate by 1 mV from the Nernstian slope, calculated using Eq. 17 and the values for the diffusion coefficients and the standard ion-transfer potentials given in Table 1. The values of diffusion coefficients for TPnA^+ and THA^+ are assumed to be the same as that for TBA^+ . The diffusion coefficient of each ion in the nitrobenzene was taken as a half of the one in aqueous solution.⁶

Effect of the Anionic Species: The effect of the counter ionic species was studied for the interface, $\text{TBAX(W)}/\text{TBATPB(NB)}$ using the cell(I) for $\text{X} = \text{Cl}^-$ ($a=1$, $b=50$, and $c=0.1-200 \text{ mmol dm}^{-3}$) and

Br^- ($a=1$, $b=10$, and $c=0.01$ — 100 mmol dm^{-3}) and also using the following cell:



for $\text{X}=\text{I}^-$. The change in l.j.p. values from the measured emf values was obtained as described above for $\text{X}=\text{Cl}^-$ and Br^- , while the l.j.p. at the interface between phases V and VI was neglected in the cell(II). The results were plotted against $\log(c_{\text{TBAX}}^{\text{W}}/c_{\text{TBATPB}}^{\text{O}})$ in Fig. 2.

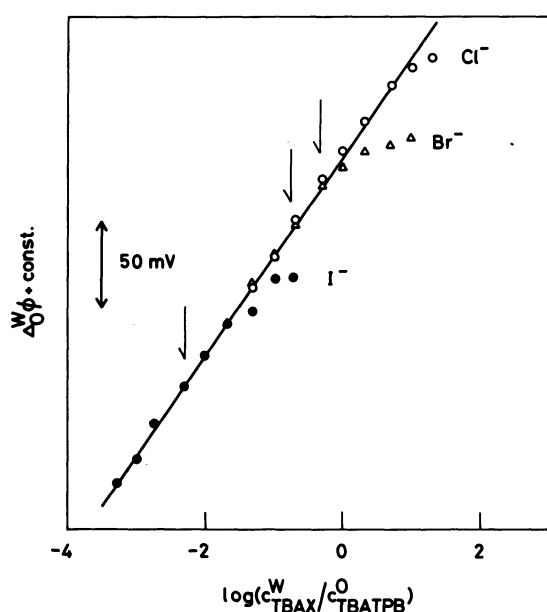


Fig. 2. Change of the liquid-junction potentials for the system: TBATPB(nitrobenzene)/TBAX(water), where R=chloride, bromide, or iodide ion.

Table 1. Standard Ion-Transfer Potentials of Ion Transfer from Water to Nitrobenzene and Diffusion Coefficients of Ions in Water

Ion	$\Delta_{\text{NB}}^{\text{W}} \varphi^0 / \text{V}^{\text{a}}$	$D / \text{cm}^2 \text{s}^{-1}^{\text{c}}$
Li^+	0.395	—
TPrA^+	-0.154 ^b	6.24×10^{-6}
TBA^+	-0.248	5.21×10^{-6}
TPnA^+	-0.343 ^b	—
TUA^+	-0.438 ^b	—
Cl^-	-0.324	2.0×10^{-5}
Br^-	-0.295	2.1×10^{-5}
I^-	-0.195	2.1×10^{-5}
TBP^-	0.372	—

a) Data in Ref. 3. b) Calculated from the data in Ref. 3. c) Calculated from the limiting equivalent conductances given in Ref. 10.

These curves were shifted vertically to superimpose the linear portions of the curves upon each other. As the radius of the counter ion increases, the curves start to deviate from the Nernstian response at the lower value of the concentration ratio, i.e., the more hydrophobic the counter ion is, the greater is the degree of interference. This is also the behavior expected from Eq. 17. The arrows in Fig. 2 indicate the points where the curves deviate by 1 mV from the Nernstian slope, calculated with Eq. 17 and the values in Table 1.

Effect of the Concentration of the Electrolyte: Equation 17 indicates that when the system $\text{K}_1\text{A}_1(\text{W})/\text{K}_1\text{A}_2(\text{O})$ functions as a liquid-membrane ion-selective electrode at a constant concentration of K_1A_2 , the concentration level of K_1A_1 where the system shows Nernstian response. Similarly, when the system works as a reference electrode reversible to the K_1 ion in the oil phase at a constant concentration, the concentration level of K_1A_1 in the aqueous phase limits the range of the Nernstian region. Such a concentration effect has great practical importance to determine the suitable conditions in designing reference electrodes and ion-selective electrodes of a liquid-membrane type.

The change of the l.j.p. for the system TBATPB(NB)/TBACl(W) was estimated from the emf values of the cell (I) for the various concentrations ($a=b/10$, $b=0.5, 1, 2, 5, 10, 20, 50$, and 100 , and $c=0.1$ — 500 mmol dm^{-3}) of TBATPB and TBACl. Figure 3 shows the response of the system with respect to the concentra-

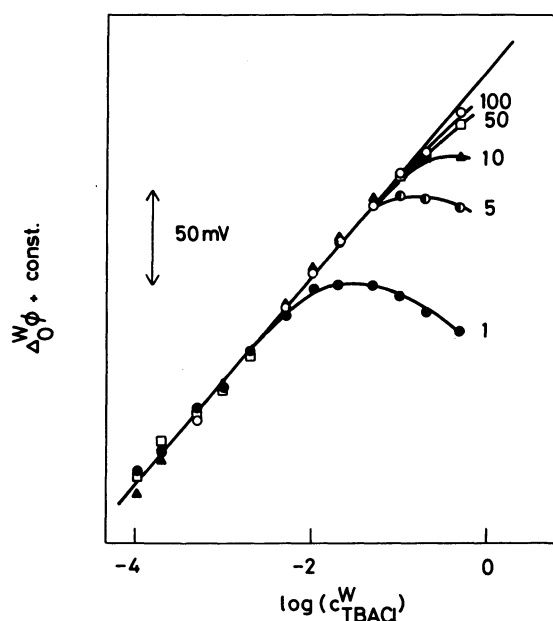


Fig. 3. Effect of the concentration of TBATPB in nitrobenzene on the change of the liquid-junction potential. Labels indicate the concentration of TBATPB in nitrobenzene in mmol dm^{-3} .

tion of TBACl at five different concentrations of TBATPB in the nitrobenzene phase. As the concentrations of TBATPB increases, the Nernstian region becomes wider. In terms of the liquid-membrane ion-selective electrodes, this means that the concentration of the "ion-exchanger" (TPB⁻ ion in the present system) in the membrane must be high in order to obtain the wider concentration range of the Nernstian response for TBACl. The curve for $b_{\text{TBATPB}}^0 = 1 \text{ mmol dm}^{-3}$ in Fig. 3 has a maximum and, in the higher concentration region, the l.j.p. changes in opposite direction with increasing concentration of TBACl. Similar tendency was found also in the curve at $b_{\text{TBATPB}}^0 = 5 \text{ mmol dm}^{-3}$. Such a tendency can be ascribed to the l.j.p. in the nitrobenzene phase caused by the migration of Cl⁻ ion in the nitrobenzene phase, as will be shown below.

Figure 4 shows the change of the l.j.p. with the mean ionic activity of TBATPB in the nitrobenzene phase, $a_{\text{TBATPB}}^{\pm, \text{NB}}$, at the three different concentrations of TBACl. The activity instead of the concentration was used in Fig. 4 to check if this system responds thermodynamically to the activity of the TBA⁺ ion. The activity coefficients of TBA⁺ and TPB⁻ ions were calculated by using the Debye-Hückel theory allowing for the finite size of the ions.¹¹⁾ At $b_{\text{TBACl}}^{\text{W}} = 1 \text{ mmol dm}^{-3}$, the change of the l.j.p. vs. $\log(a_{\text{TBATPB}}^{\pm, \text{NB}})$

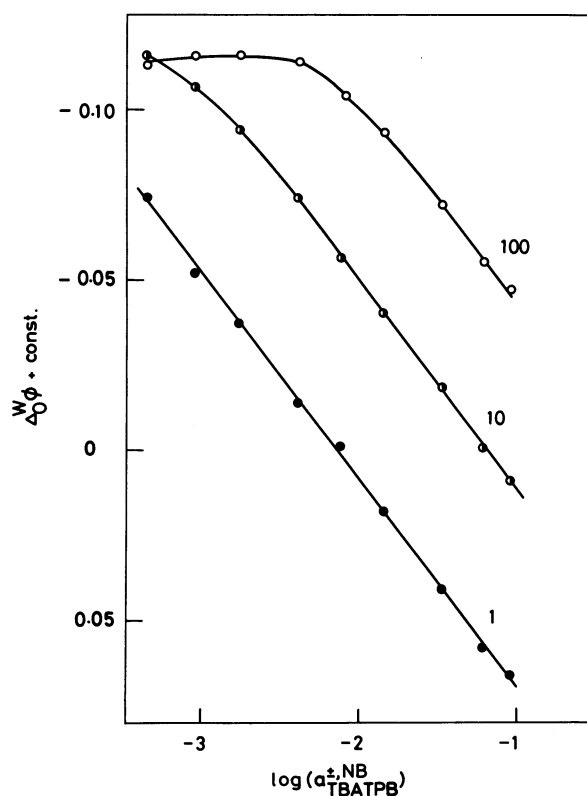


Fig. 4. Effect of the concentration of TBACl in aqueous solution on the change of the liquid-junction potential. Labels indicate the concentration of TBACl in aqueous phase in mmol dm^{-3} .

plot was linear with the slope of 60 mV per decade change of $a_{\text{TBATPB}}^{\pm, \text{NB}}$ in the whole concentration range studied ($0.5\text{--}100 \text{ mmol dm}^{-3}$). This indicates that the present system can be employed as a reference electrode reversible to the TBA⁺ ion in the nitrobenzene phase in this concentration range. At $b_{\text{TBACl}}^{\text{W}} = 10 \text{ mmol dm}^{-3}$ the curve in Fig. 4 deviated from the Nernstian slope in the lower concentration (activity) region of TBA⁺ ion. The deviation occurred at much higher concentration (activity) region when $b_{\text{TBACl}}^{\text{W}} = 100 \text{ mmol dm}^{-3}$. These results indicate that the concentration of TBACl must be kept as small as possible to obtain a wider range of Nernstian response. This type of the interface has been successfully used at $b_{\text{TBACl}}^{\text{W}} = 5 \text{ mmol dm}^{-3}$ as a reference electrode in studying the specific adsorption of TBA⁺ and TPB⁻ ions at the nitrobenzene-water interface by using electrocapillary measurements.¹²⁾

Nitrobenzene-Water Interface Reversible to Tetraphenylborate Ion. It is sometimes convenient to use a reference electrode reversible to an anion instead of a cation dissolved in organic phase. For example, to study thermodynamically the specific adsorption of cations in the nitrobenzene, one must use a reference electrode reversible to the anion in the nitrobenzene phase. In addition, when a cation in the oil phase is very hydrophobic, i.e., in the case $\Delta_O^{\text{W}} \phi_{\text{K}1}^0 \leq \Delta_O^{\text{W}} \phi_{\text{A}1}^0$, one has to keep the ratio $b_{\text{K}1\text{A}2}^0 / b_{\text{K}1\text{A}1}^0$ large enough to ensure the Nernstian response of the interface if one uses a cation reversible reference electrode. In such cases, the anion reversible reference electrode is promising. We examined the possibility of the nitrobenzene-water interfaces reversible to the TPB⁻ ion by measuring the emf of the following cells:

I	II	III	IV	V
Ag	AgCl	1 mM LiCl (W)	1 mM LiTPB (W)	$a \text{ M}$ TPnATPB (NB)
		VI	VII	VIII
		$a/10 \text{ M}$ LiTPB (W)	$a/10 \text{ M}$ LiCl (W)	AgCl
				IX
				Ag (IV)

for TPnA⁺ ($a = 5\text{--}200 \text{ mmol dm}^{-3}$) and

I	II	III	IV	V
Ag	AgCl	0.5 mM LiCl (W)	0.5 mM LiTPB (W)	$a \text{ M}$ THATPB (NB)
		VI	VII	VIII
		$a \text{ M}$ TPrATPB (NB)	$a \text{ M}$ TPrACl (W)	AgCl
				IX
				Ag (V)

for THA^+ ($a=5-40 \text{ mmol dm}^{-3}$).

Since in the cell (IV) the ratio $b_{\text{TPnATPB}}^{\text{NB}}/b_{\text{LiTPB}}^{\text{W}}$ was kept constant during the change of $b_{\text{TPnATPB}}^{\text{NB}}$, the change of the potential difference between the phases V and VI with $b_{\text{TPnATPB}}^{\text{NB}}$ can be considered negligible. Similarly, the change in the potential difference between the phases VI and VII is also negligible. The changes in the potential falls between phases VII and VIII in the cells (IV) and (V) with $b_{\text{RCI}}^{\text{W}}$ ($\text{R}=\text{Li}^+$ or TPnA^+) were allowed for as described above. The changes of the l.j.p.'s which reside between the phases VI and VII in the cell (IV) and between the phases V and VI in the cell (V) were neglected, because the change of the ratio of the equivalent conductances for THATPB and TPnATPB in the nitrobenzene phase with the change of the electrolyte concentration and also that for LiTPB and LiCl in the aqueous phase seem negligibly small. The changes of the l.j.p.'s across the phases IV and V in the cell (IV) and (V) thus estimated are plotted against $\log(a_{\text{RTPB}}^{\pm, \text{NB}})$ in Fig. 5. Both interfaces respond linearly with the slope of 58 mV(TPnA^+) and 60 mV(THA^+) within the concentration range studied. Thus, the system LiTPB (W)/ RTPB (NB) can be used as a reference electrode reversible to the TPB^- ion in the nitrobenzene phase. This type of reference electrode has been applied in studying the specific adsorption of cationic surfactants at the nitrobenzene-water interface by using the mixed electrolyte method.¹³⁾

Significance of the Diffusion Potential. Figure 3 shows that the curves at $b_{\text{TBATPB}}^{\text{O}}=1$ and 5 mmol dm^{-3} have maxima. The approximate theoretical treatment of the l.j.p. described above can predict the concentration at which the l.j.p. starts to deviate from

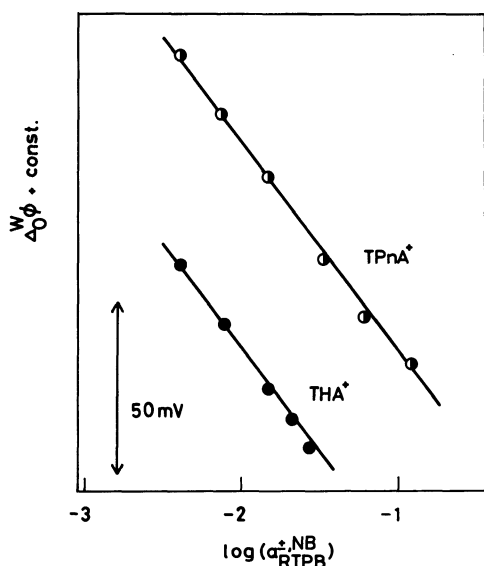
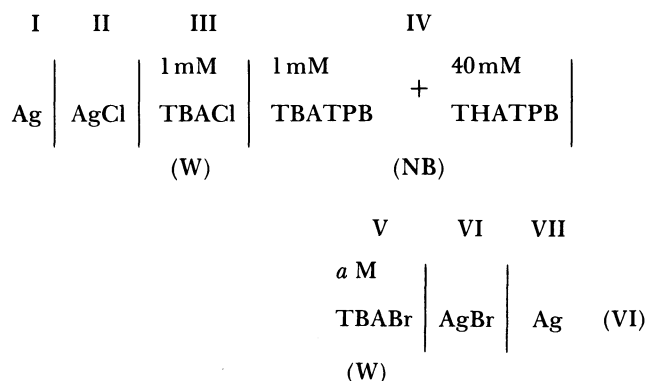


Fig. 5. Change of the liquid-junction potentials for the system: RTPB (nitrobenzene), LiTPB (water), where $\text{R}=\text{TPnA}^+$ or THA^+ ion.

the Nernstian response, but cannot explain the inversion of the slope. In fact, Eq. 17 gives a constant value of $\Delta\phi_{\text{interfacial}, i=0}^{\text{W}}$ when $b_{\text{K1A2}}^{\text{O}}/b_{\text{K1A1}}^{\text{W}} \rightarrow \infty$. The approximation introduced previously is obviously not adequate in such a high concentration region, since a significant amount of Cl^- ion enters into the nitrobenzene phase, so that its amount is no longer negligible in the vicinity of the interface. The diffusion coefficient of Cl^- ion is probably much larger than those of TBA^+ and TPB^- ions in the nitrobenzene phase (cf. Table 1). Therefore, the positive diffusion potential (the potential is referred to that at the infinity of the nitrobenzene phase), which is opposite in sign to that of the interfacial potential, will develop in the vicinity of the interface.

If this diffusion potential is responsible to the inversion of the potential, the addition of a supporting electrolyte in the nitrobenzene phase should suppress the l.j.p. in that phase, resulting in the disappearance of the maximum. The emf of the following cell was measured with and without 40 mmol dm^{-3} THATPB .



The change in the potential drop between the phases V and VI was allowed for as described above.

Figure 6 shows the change of the l.j.p. vs. $\log(b_{\text{TBABr}}^{\text{W}}/b_{\text{TBATPB}}^{\text{O}})$ curves. The curve for the cell without THATPB (Curve 1 in Fig. 6) exhibited a maximum at $\log(b_{\text{TBATPB}}^{\text{O}}/b_{\text{TBABr}}^{\text{W}}) \approx 1$ and decreased with the further increase of $b_{\text{TBABr}}^{\text{W}}$. This inverted change of the l.j.p. was almost eliminated by adding 40 mmol dm^{-3} THATPB to the nitrobenzene phase, as is shown in Curve 2 in Fig. 6. The slight decrease at the highest concentration is probably due to an insufficient concentration of THATPB to eliminate fully the migration of the Cl^- ion. This experiment clearly indicates the significant contribution of the diffusion potential in the nitrobenzene phase to the inversion of the slope shown in Curve 1 in Fig. 6. To confirm further the effect of the diffusion potential, the diffusion-migration equations were solved numerically using a finite difference method¹⁴⁾ without introducing the assumption given by Eq. 2. The values given in Table 1 were used for the calculation. The result for the system TBABr (W)/ TBATPB (NB) is

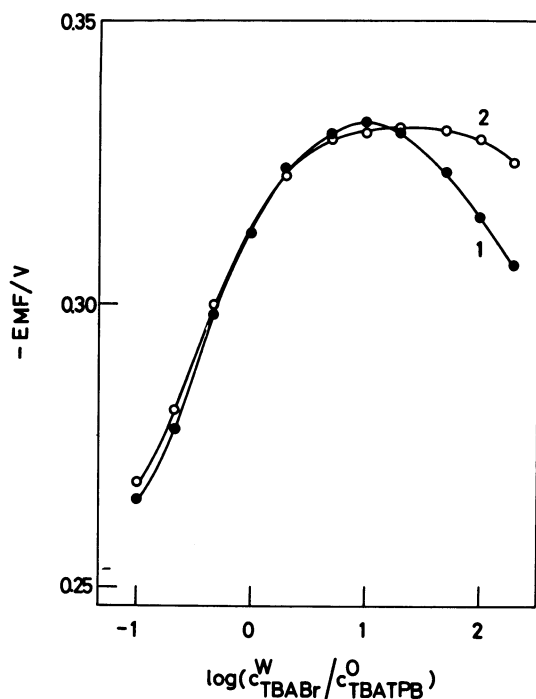


Fig. 6. Change of the liquid-junction potential for the system: TBATPB(nitrobenzene)/TBABr(water), in the presence of (Curve 2) and the absence of (Curve 1) 40 mmol dm⁻³ THATPB in nitrobenzene as a supporting electrolyte.

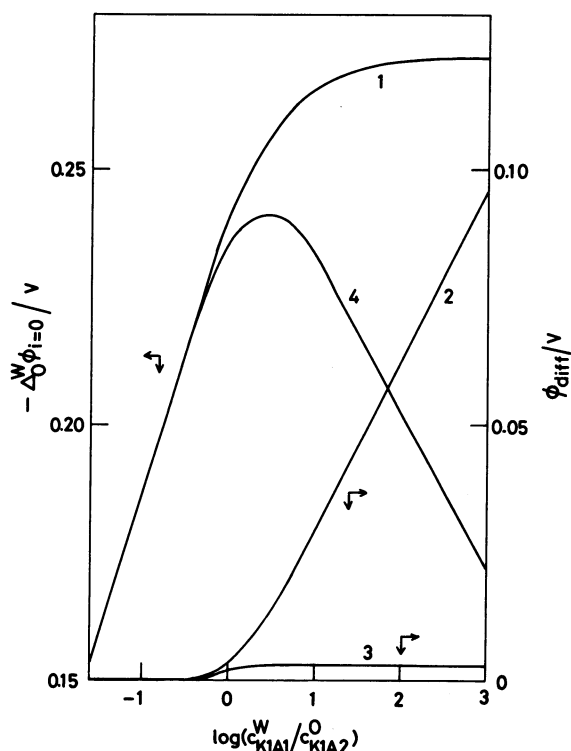


Fig. 7. Calculated values of the interfacial potential (Curve 1), the diffusion potential in nitrobenzene phase (Curve 2), the diffusion potential in aqueous phase (Curve 3), and the total liquid-junction potential (Curve 4) for the system: TBATPB(nitrobenzene)/TBABr(water).

given in Fig. 7.

In the higher concentration region, the interfacial potential (Curve 1) reached a limiting value. Simultaneously, the diffusion potential in the nitrobenzene phase (Curve 2) increases linearly with the logarithm of the concentration ratio, while the diffusion potential in the aqueous phase (Curve 3) stays at a nominal value. Accordingly, the total liquid-junction potential (Curve 4) possesses a maximum and beyond this point the potential in turn decreases linearly with the concentration. Thus, although the contribution of the diffusion potential seems smaller in the actual system if one compares Fig. 6 with Fig. 7, the numerical calculation essentially reproduces the experimental trend, indicating the importance of the diffusion potential in the concentration range far from the Nernstian response.

Such a contribution of the diffusion potential to the measured emf value may have a practical importance. Liquid-ion exchange membrane ion-selective electrodes have been used to determine the critical micelle concentration of ionic surfactants by making use of the intersection point of the two linear portion of the emf vs. logarithm of the surfactant concentration curve.^{15,16} The results in Figs. 6 and 7 indicate that such a method for determining the critical micelle concentration (cmc) may lead to a spurious conclusion. Disagreement has been reported between the cmc value determined from another method and the value from the concentration of the intersection point in the emf vs. the logarithm of the surfactant concentration curve.^{17,18}

Appendix 1

From Eq. 1, we may write for the flux of the ions in oil phase

$$f_{\text{K1}}^{\text{O}} = -D_{\text{K1}}^{\text{O}} \frac{\partial c_{\text{K1}}^{\text{O}}}{\partial x} - \frac{F}{RT} D_{\text{K1}}^{\text{O}} c_{\text{K1}}^{\text{O}} \frac{\partial \phi^{\text{O}}}{\partial x}, \quad (\text{A1})$$

$$f_{\text{A1}}^{\text{O}} = -D_{\text{A1}}^{\text{O}} \frac{\partial c_{\text{A1}}^{\text{O}}}{\partial x} + \frac{F}{RT} D_{\text{A1}}^{\text{O}} c_{\text{A1}}^{\text{O}} \frac{\partial \phi^{\text{O}}}{\partial x}, \quad (\text{A2})$$

$$f_{\text{A2}}^{\text{O}} = -D_{\text{A2}}^{\text{O}} \frac{\partial c_{\text{A2}}^{\text{O}}}{\partial x} + \frac{F}{RT} D_{\text{A2}}^{\text{O}} c_{\text{A2}}^{\text{O}} \frac{\partial \phi^{\text{O}}}{\partial x}. \quad (\text{A3})$$

On the other hand, the current density I in oil phase is represented by

$$I = F(f_{\text{A1}}^{\text{O}} + f_{\text{A2}}^{\text{O}} - f_{\text{K1}}^{\text{O}}). \quad (\text{A4})$$

Substituting (A1), (A2), and (A3) into (A4), $\partial \phi^{\text{O}}/\partial x$ can be represented by

$$\frac{\partial \phi^{\text{O}}}{\partial x} = -\frac{RT}{F} Z, \quad (\text{A5})$$

where

$$Z = (D_{\text{K1}}^{\text{O}} \frac{\partial c_{\text{K1}}^{\text{O}}}{\partial x} - D_{\text{A1}}^{\text{O}} \frac{\partial c_{\text{A1}}^{\text{O}}}{\partial x} - D_{\text{A2}}^{\text{O}} \frac{\partial c_{\text{A2}}^{\text{O}}}{\partial x} + \frac{I}{F})/\beta$$

and

$$\beta = D_{K1}^0 c_{K1}^0 + D_{A1}^0 c_{A1}^0 + D_{A2}^0 c_{A2}^0.$$

When $D_{K1}^0 + c_{K1}^0 + D_{A2}^0 c_{A2}^0 \gg D_{A1}^0 c_{A1}^0$, after substituting Eq. A5 into A1, A2, and A3, we obtain

$$f_{K1}^0 = -\mathcal{D}_1^0 \frac{\partial c_{K1}^0}{\partial x} - \mathcal{D}_2^0 \frac{\partial c_{A1}^0}{\partial x} + t_{K1}^0 \frac{I}{F} \quad (A6)$$

and

$$f_{A1}^0 = -D_{A1}^0 \frac{\partial c_{A1}^0}{\partial x}, \quad (A7)$$

where \mathcal{D}_1^0 and \mathcal{D}_2^0 are given by Eqs. 5 and 6.

Appendix 2

Solving the differential equations, Eqs. 7–9, under the initial and boundary conditions, Eqs. 10–16, we obtain, when $D_{A1}^0 \neq \mathcal{D}_1^0$

$$\begin{aligned} c_{K1}^0(x, t) = & b c_{K1A2}^0 + \left(pA - \frac{\mathcal{D}_2^0}{D_{A1}^0 - \mathcal{D}_1^0} qA \right. \\ & \left. - b c_{K1A2}^0 \right) \operatorname{erfc} \left[-\frac{x}{2(\mathcal{D}_1^0 t)^{1/2}} \right] \\ & + \frac{\mathcal{D}_2^0}{D_{A1}^0 - \mathcal{D}_1^0} qA \operatorname{erfc} \left[-\frac{x}{2(D_{A1}^0 t)^{1/2}} \right] \end{aligned} \quad (A8a)$$

and

$$c_{A1}^0(x, t) = qA \operatorname{erfc} \left[-\frac{x}{2(D_{A1}^0 t)^{1/2}} \right], \quad (A9)$$

where p , q , and A are given by Eqs. 15, 16, and 24, respectively. When $D_{A1}^0 = \mathcal{D}_1^0$, instead of Eq. A1, we have

$$\begin{aligned} c_{K1}^0(x, t) = & b c_{K1A2}^0 - \frac{\mathcal{D}_2^0}{2(\mathcal{D}_1^0)^{3/2}} qAx \frac{1}{(\pi t)^{1/2}} \exp \left(-\frac{x^2}{4t\mathcal{D}_1^0} \right) \\ & + (pA - b c_{K1A2}^0) \operatorname{erfc} \left[-\frac{x}{2(\mathcal{D}_1^0 t)^{1/2}} \right]. \end{aligned} \quad (A8b)$$

On the other hand, for $c_{K1}^w(x, t)$ we have

$$c_{K1}^w(x, t) = b c_{K1A1}^w + A \operatorname{erfc} \left[\frac{x}{2(\mathcal{D}_w^0 t)^{1/2}} \right]. \quad (A10)$$

From Eqs. A4, A8, A9, and A10, the current-potential relationship can be written as:

$$\frac{I}{F} = -\frac{1}{(\pi t)^{1/2}} \frac{1}{t_{A1}^w} A [Np + (M - (D_{A1}^0)^{1/2} q) - N b c_{K1A2}^0], \quad (A11)$$

where M and N are given by Eqs. 26 and 27. This equation is valid irrespective of the magnitude of D_{A1}^0 and \mathcal{D}_1^0 . Setting $I=0$ in Eq. A11, we obtain Eq. 17.

Under the conditions of Eq. 2 and at $I=0$ we may write from Eq. 1,

$$\frac{\partial \varphi}{\partial x} = \frac{RT}{F} \frac{D_{A2}^0 - D_{K1}^0}{D_{K1}^0 + D_{A2}^0} \frac{\partial \ln c_{K1}^0}{\partial x}. \quad (A12)$$

Integrating this equation from $x=-\infty$ to $x=0$, we have

$$\varphi(x=0) - \varphi(x=-\infty) = \frac{RT}{F} (1 - 2t_{K1}^0) \ln \frac{c_{K1}^0(0, t)}{b c_{K1A2}^0} \quad (A13)$$

Substituting Eq. A8 at $x=0$, we obtain Eq. 23. Eq. 24 can be derived similarly.

This work was supported by Grant-in-Aids for Scientific Research No. 60211017 from the Ministry of Education and Culture.

References

- 1) a) M. Senda, T. Kakutani, and T. Osakai, *Denki Kagaku*, **49**, 322 (1981). b) J. Koryta and P. Vanysek, *Advances in Electrochemistry and Electrochemical Engineering*, ed by H. Gerischer and C. W. Tobias, John Wiley, New York (1981), Vol. 12, p. 113.
- 2) E. A. Guggenheim, "Thermodynamics," 6th ed, North-Holland, Amsterdam (1977), p. 307.
- 3) L. Q. Hung, J. *Electroanal. Chem. Interfacial Electrochem.*, **115**, 159 (1980).
- 4) T. Kakiuchi and M. Senda, *Bull. Chem. Soc. Jpn.*, **57**, 1801 (1984).
- 5) T. Osakai, T. Kakutani, and M. Senda, *Bull. Chem. Soc. Jpn.*, **57**, 370 (1984).
- 6) T. Kakiuchi and M. Senda, *Bull. Chem. Soc. Jpn.*, **56**, 1322 (1983).
- 7) R. W. Kunze and R. M. Fuss, *J. Phys. Chem.*, **67**, 385 (1963).
- 8) E. D. Schall, *Anal. Chem.*, **29**, 1044 (1957).
- 9) C. Davies, "Ion Association," Butterworth, London (1962), p. 39.
- 10) R. A. Robinson and R. H. Stokes, "Electrolyte Solutions," Butterworth, London (1959), p. 463.
- 11) H. S. Harned and B. B. Owen, "Physical Chemistry of Electrolyte Solutions," 3rd ed, Reinhold, New York (1958), p. 731.
- 12) T. Kakiuchi and M. Senda, *Bull. Chem. Soc. Jpn.*, **56**, 1753 (1983).
- 13) T. Kakiuchi, M. Kobayashi, and M. Senda, *Bull. Chem. Soc. Jpn.*, **60**, 3109 (1987).
- 14) S. W. Feldberg, "Electroanalytical Chemistry," ed by A. Bard, Marcel Dekker (1969), Vol. 3, p. 199.
- 15) C. Cavach and C. Bertrand, *Anal. Chim. Acta*, **55**, 385 (1971).
- 16) N. Ishibashi and H. Ohara, *Bunseki Kagaku*, **21**, 100 (1972).
- 17) B. J. Birch and D. E. Clarke, *Anal. Chim. Acta*, **61**, 159 (1972).
- 18) H. Hara, S. Okazaki, and T. Fujinaga, *Nippon Kagaku Kaishi*, **1980**, 1645.